Syntheses, structural characterisation and magnetic properties of Fe(II) and Mn(II) compounds with the pentacyanopropenido ligand; structural characterisation of a substituted pyrazolo[1,5-*a*]pyrimidine†

Emeric Lefebvre,[a] Françoise Conan,*[a] Nathalie Cosquer,[a] Jean-Michel Kerbaol,[a] Mathieu Marchivie,[a] Jean Sala-Pala,[a] Marek M. Kubicki,[b] Estelle Vigier[b] and Carlos J. Gomez Garcia[c]

Received (in Montpellier, France) 6th April 2006, Accepted 9th June 2006
First published as an Advance Article on the web 27th June 2006
DOI: 10.1039/b605030a

Reactions between the metal(II) salts $[M(CH_3CN)_n](BF_4)_2$ (M = Fe, n = 6; M = Mn, n = 4) and some organic anionic polynitriles were studied. With the pentacyanopropenide anion pcp^- [pcp^- = $(NC)_2CC(CN)C(CN)_2^-$], were obtained, according to the experimental conditions, the new complexes $[M(pcp)_2(H_2O)_4]$ (**1**, M = Fe; **2**, M = Mn) and $[M(pcp)_2]$ (**3**, M = Fe; **4** = Mn). Use of the hexacyano-3,4-diazahexadienediide anion $[(NC)_2CC(CN)NNC(CN)C(CN)_2^{2-}]$ instead of pcp^- did not afford polynitrile metal complexes but led to a new organic derivative **5**, of formula $C_{10}N_8H_2$. Crystallographic studies indicated that the isostructural compounds **1** and **2** involve discrete monomeric units with pcp ligands acting with a monodentate coordination mode and having the metal in a pseudooctahedral *trans*-MN_2O_4 environment; however, a rich hydrogen bond system gives rise to a 3D array. Complex **3**, which presents metal in a pseudooctahedral MN_6 environment, has a 3D structure arising from pcp ligands having an unprecedented μ_3-coordination mode. Compound **5** is a bicyclic derivative with a pyrazolo[1,5-*a*]pyrimidine skeleton. In all derivatives, the organic part is essentially planar and involves a strongly delocalized π system. The magnetic properties of the inorganic complexes have been studied in the 2–300 K range. Fit of the magnetic data indicates high spin complexes with weak antiferromagnetic interactions in **2**, **3** and **4** and the presence of a significant zero field splitting of the Fe(II) ion in **1**.

Introduction

Organic polynitrile derivatives are fascinating units since, associated with inorganic entities, many of them may lead to a wide variety of molecular arrangements that mostly display significant physical properties in the field of magnetism and electrical conduction.[1–6]

Among these polynitrile units, the highly conjugated cyanocarbanions or azacyanocarbanions, synthesised from tetracyanoethylene TCNE (Scheme 1)],[7–8] catch our attention [9–14] for geometrical and electronic reasons: (i) despite the presence of various CN groups, their geometry precludes the possibility of a chelate coordination mode and they can only act as bridging ligands affording polymeric compounds, and (ii) association of the π electronic system of the CN groups with the π system of the skeleton induces high electronic delocalisation and should allow transmission of electronic effects between the metal centers.

Following these general arguments, our objective is to examine the ability of these organic ligands to create a range of 1D, 2D and 3D polymeric assemblies. In this paper, we present some results obtained with the pentacyanopropenide [pcp^- = $(NC)_2CC(CN)C(CN)_2^-$] and the hexacyano-3,4-diazahexadienediide [$(NC)_2CC(CN)NNC(CN)C(CN)_2^{2-}$ = $C_{10}N_8^{2-}$] anions. While results concerning the latter remain scarce],[7,12] previous studies have shown that, in inorganic derivatives, the pcp group is a very versatile moiety which may act either as a simple counterion or as a N ligand able to present different coordination modes.[13,15–21] As for example, while it acts in complexes $[M(pcp)(PPh_3)_3]$ (M = Cu, Ag) as a unidentate ligand,[18] it presents μ_2- and μ_4-coordination modes in $[M(pcp)(PPh_3)_2]$ (M = Cu, Ag) and [Ag(pcp)], respectively.[19–20] We report herein the syntheses, crystal structures and magnetic properties of new Fe(II) and Mn(II) derivatives of formula $[M(pcp)_2(H_2O)_4]$ and $[M(pcp)_2]$. Similar reactions using the $C_{10}N_8^{2-}$ anion (Scheme 1) instead of pcp^- did not afford polynitrile metal complexes but interestingly led to a new organic derivative, of formula $C_{10}N_8H_2$, whose structure, built on a pyrazolo[1,5-a]pyrimidine skeleton, is also presented on the basis of crystallographic results.

[a] *Laboratoire de Chimie, Electrochimie Moléculaires et Chimie Analytique, UMR CNRS 6521, Université de Bretagne Occidentale, CS 93837, 29238 Brest-Cedex 3, France. E-mail: francoise.conan@univ-brest.fr.*
[b] *Laboratoire de Synthèse et d'Electrosynthèse Organométalliques, UMR CNRS 5632, Université de Bourgogne, 21000 Dijon, France*
[c] *Instituto de Ciencia Molecular, Universidad de Valencia, 46100 Burjassot, Spain*

† The HTML version of this article has been enhanced with colour images.

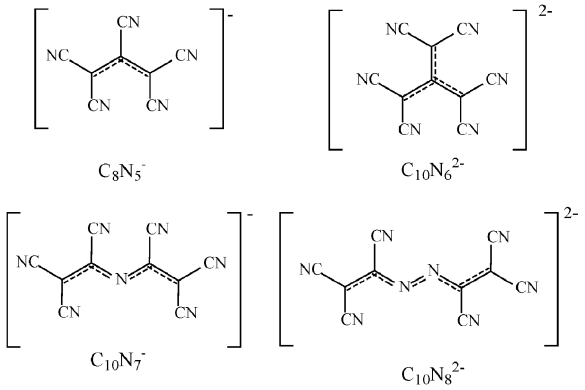

Scheme 1

Experimental

General

Solvents were distilled using standard techniques and were thoroughly deoxygenated before use. Elemental analyses were performed by the "Service Central d'Analyses du CNRS", Vernaison, France. IR spectra were obtained with a Nicolet Nexus spectrometer (KBr pellets). ESR spectra were run on a Bruker Elaxys spectrometer (X-band). The starting materials $[Fe(CH_3CN)_6](BF_4)_2$,[22] $[Mn(CH_3CN)_4](BF_4)_2$,[22] $Et_4N(C_8N_5)$[7,13] and $(Et_4N)_2(C_{10}N_8)$[7,12] were prepared as described in the literature.

Syntheses and general characterizations

Compounds $[M(C_8N_5)_2(H_2O)_4]$ (M = Fe, 1; M = Mn, 2)

*$[Fe(C_8N_5)_2(H_2O)_4]$ (**1**).* Addition of $Et_4N(C_8N_5)$ (301 mg, 1.02 mmol) to an acetone solution (50 mL) of $[Fe(CH_3CN)_6](BF_4)_2$ (200 mg, 0.42 mmol) afforded a red solution. After reflux (*ca.* 18 h), the solution was kept at −20 °C overnight. After evaporation, the solution was reduced to dryness under low pressure. The resulting orange solid was then dissolved in methylisobutylketone (30 mL); slow diffusion of hexane in this solution afforded red single crystals suitable for X-ray analysis. Yield 30 mg (15%). Found: C, 41.3; H, 1.8; N, 30.6%. Calc. for $C_{16}H_8FeN_{10}O_4$: C, 41.8; H, 1.8 N, 30.4%. ν_{max}/cm^{-1} 3420s,br (OH), 2239w and 2215s (CN), 1644m (OH),1506s.

*$[Mn(C_8N_5)_2(H_2O)_4]$ (**2**).* An essentially similar procedure was followed using $[Mn(CH_3CN)_4](BF_4)_2$ (260 mg, 0.66 mmol) and $Et_4N(C_8N_5)$ (392 mg, 1.32 mmol) in an EtOH–H_2O mixture (60 + 3 mL) (reflux for *ca.* 72 h). The resulting solid was dissolved in acetone; slow diffusion of hexane in this solution afforded orange single crystals suitable for X-ray analysis. Yield 125 mg (31%). Found: C, 41.0; H, 1.8; N, 29.8.%. Calc. for $C_{16}H_8MnN_{10}$: C, 41.8; H, 1.8 N, 30.5%. ν_{max}/cm^{-1} 3407 vs, br (OH), 2251vw, 2228sh, 2209s (CN), 1625m, 1504s.

Compounds $[M(C_8N_5)_2]$ (M = Fe, 3; M = Mn, 4)

*$[Fe(C_8N_5)_2]$ (**3**).* This reactions was carried out in a dry box with reactants carefully dried under vacuum before use. To dichloromethane (25 mL) were added $[Fe(CH_3CN)_6](BF_4)_2$ (100 mg, 0.21 mmol) and $Et_4N(C_8N_5)$ (125 mg, 0.42 mmol). After stirring at r.t. for *ca.* 14 h, the resulting precipitate was filtered, washed with dichloromethane (2 × 10 mL) and dried under vacuum. Yield: 45 mg (75%). Orange single crystals were obtained by slow diffusion of hexane in an acetone solution of this solid; they quickly decompose due to a strong affinity towards water. Found: C, 48.4; H, 0.7, N, 33.1%. Calc. for $C_{16}FeN_{10}\cdot 0.25(CH_3)_2CO\cdot 0.75H_2O$: C, 48.3; H, 0.7; N, 33.7%. ν_{max}/cm^{-1} 2237sh and 2213s (CN), 1506s.

*$[Mn(C_8N_5)_2]$ (**4**).* Similar procedure starting from $[Mn(CH_3CN)_4](BF_4)_2$ (250 mg, 0.64 mmol) and $Et_4N(C_8N_5)$ (382 mg, 1.29 mmol). **4** was obtained as yellow microcrystals but all attempts to obtain crystals suitable for X-ray studies failed. Yield 150 mg (60%). Found: C, 46.6; Mn, 12.6; N, 32.2%. Calc. for $C_{16}MnN_{10}\cdot 0.5CH_2Cl_2$: C, 46.1; Mn, 12.8, N, 32.6%. ν_{max}/cm^{-1} 2234w, 2219s (CN), 1505s.

*Compound $C_{10}N_8H_2$ (**5**).* CH_2Cl_2 (30 mL) was poured in a flask containing $[Fe(CH_3CN)_6](BF_4)_2$ (207 mg, 0.44 mmol) and $(Et_4N)_2(C_8N_{10})$ (209 mg, 0.44 mmol). The mixture was stirred at r.t. overnight. The suspension color varied from bright orange to brown. After decantation, the dichloromethane solution was filtered off and the dark brown solid was washed three times with CH_2Cl_2 (3 × 10 mL). The organic crops were collected altogether, washed with water in a separating funnel and then were dried over $MgSO_4$. Dichloromethane was removed under low pressure. The resulting yellow powder was filtered and dried under vacuum. Yield: 29 mg (29%). Single crystals of **5** were obtained by recrystallisation either in dichloromethane or acetone. Found: C, 51.9; H, 2.2; N, 42.7%. Calc. for $C_{10}H_2N_8\cdot 0.5(CH_3)_2CO$: C, 52.4; H, 1.9; N, 42.6%. ν_{max}/cm^{-1} 3382m, 3332m, 3244m, 3207m (NH), 2239s (CN). δ_C (100 MHz; $(CD_3)_2CO$) 84.4 (C6), 98.2 (C2), 108.7, 110.4, 111.2, 111.4 (C7–C10), 128.3 (C3), 134.2 (C5), 152.1 (C4), 157.2 (C1). The labeling of the carbon atoms in is that given in Fig 7.

Crystallographic data and structure determinations

Single crystals of **1**, $\mathbf{3}\cdot 0.5(CH_3)_2CO$, **5** and $\mathbf{5}\cdot(CH_3)_2CO$ suitable for X-ray studies were mounted on an Oxford Diffraction Xcalibur diffractometer; **2** was studied using a Nonius Kappa CCD diffractometer. The unit cell determinations and data collections were carried out with Mo-Kα radiation (λ = 0.710 73 Å).

For compound **2**, the measured intensities were reduced with the DENZO program.[23] The structure was solved *via* direct methods with SHELXS97 and further refined with full-matrix least-squares methods (SHELXL97) based on $|F^2|$.[24] All non-hydrogen atoms were refined with anisotropic thermal parameters. The hydrogen atoms in **1** and **2** were found from difference Fourier maps and isotropically refined. However for **1**, OH bond lengths were constrained.

For compounds **1**, $\mathbf{3}\cdot 0.5(CH_3)_2CO$, **5** and $\mathbf{5}\cdot(CH_3)_2CO$, the unit cell determination and data reduction were performed using the CrysAlis program suite [25] on the full set of data. The structure was solved with either SIR-97 software[26] or SHELXS97 and refined using the SHELXL97 program.[24] Both software were used within the WINGX package.[27]

For $3 \cdot 0.5(CH_3)_2CO$, a small crystal (0.15 × 0.15 × 0.1 mm^3) was used to collect the full sphere of data. In order to isolate it from wet air, it has been immersed in a drop of Nujol® before being cooled down to 170 K. In these conditions, the crystal provided a weak, but usable, diffraction pattern. The full sphere data collection was then performed using 0.75° φ-scans and ω-scans with an exposure time of 40 s per frame. No absorption correction was needed owing to the low absorption coefficient. The relatively high R_{int} value and consequently high R and $wR2$ quality factors are very likely due to the bad quality of the crystal which is air sensitive and to the presence of a distorted solvent molecule within the structure. The acetone molecule shows two statistical positions (the C atom of the carbonyl group acts as an inversion centre) with an occupancy factor of 1/4; in this way, the acetone molecule alternates both positions every four cells. The hydrogen atoms of this molecule were not introduced in the refinement. Crystallographic data and final discrepancy factors are gathered in Table 1.

CCDC reference numbers 610446–610450.

For crystallographic data in CIF or other electronic format see DOI: 10.1039/b605030a

Magnetic measurements

The solid state magnetic susceptibility measurements were carried out on powder samples using a Gouy balance (Johnson Matthey) at room temperature. Variable temperature susceptibility measurements were carried out in the temperature range 2–300 K at an applied magnetic field of 0.1 T on polycrystalline samples with a Quantum Design MPMS-XL-5 SQUID magnetometer. The susceptibility data were corrected for the sample holder previously measured using the same conditions and for the diamagnetic contributions of the salt as deduced by using Pascal's constant tables.

Results and discussion

Syntheses and characterization of the inorganic complexes

Reactions of the tetraethylammonium salt of the pentacyanopropenide anion [$pcp^- = (NC)_2CC(CN)C(CN)_2^-$] (Scheme 1) with different acetonitrile first-row transition metal complexes $[M(CH_3CN)_n](BF_4)_2$ (M = Mn, Fe, Ni and Cu) were studied. In all cases, metathesis reactions associated with the bonding of the anion to the metal centre occurred as clearly evidenced by IR analyses (*vide infra*). While problems were encountered with the purification of the Ni and Cu derivatives, new compounds were obtained with Mn and Fe. According to the experimental conditions (Experimental section), hydrated $[M(pcp)_2(H_2O)_4]$ (**1**, M = Fe; **2**, M = Mn) and non-hydrated $[M(pcp)_2]$ complexes (**3**, M = Fe; **4** = Mn) were obtained. The IR spectra of compounds **1–4** clearly exhibit the usual ν_{CN} vibration bands typical of the cyano groups in the 2100–2300 cm^{-1} range; significant increases in the wavenumbers with respect to the anion (2239 and 2215 cm^{-1} for **1**, 2201 cm^{-1} for $Et_4N(C_8N_5)$) indicate coordination of the polynitrile unit to the metal centre.[28] The IR spectra of hydrated complexes **1–2** also exhibit absorption bands arising from the presence of water (at *ca.* 3400 and 1640 cm^{-1}, respectively for ν_{OH} and δ_{HOH}).

Crystal structures of the inorganic complexes

The metal environment. Compounds **1** and **2** are isostructural; both crystallise in the monoclinic system, space group $P2_1/c$ (Table 1). In each case, the asymmetric unit consists of one metallic atom located on a special position (000), a polynitrile unit and two water molecules in general positions. This leads to a centrosymmetric $[M(C_5N_8)_2(H_2O)_4]$ molecule, in which the metal presents a pseudo-octahedral coordination arising from a $[(CN)_2CC(CN)C(CN)_2]$ ligand which acts with a monodentate coordination mode (Fig. 1). The deformation

Table 1 Crystal data and structure refinement for compounds **1**, **2**, $3 \cdot 0.5(CH_3)_2CO$, **5** and $5 \cdot (CH_3)_2CO$

	1	**2**	$3 \cdot 0.5(CH_3)_2CO$	**5**	$5 \cdot (CH_3)_2CO$
Empirical formula	$C_{16}H_8FeN_{10}O_4$	$C_{16}H_8MnN_{10}O_4$	$C_{17.5}H_3FeN_{10}O_{0.5}$	$C_{10}H_2N_8$	$C_{13}H_8N_8O$
M	460.17	459.26	414.13	234.2	292.27
Crystal system	Monoclinic	Monoclinic	Orthorhombic	Monoclinic	Orthorhombic
Space group	$P2_1/c$	$P2_1/c$	$Pbca$	$P2_1/n$	$P2_12_12_1$
a/Å	5.4044(6)	5.4059(2)	11.140(3)	8.852(2)	6.352(2)
b/Å	10.449(2)	10.5483(3)	11.497(3)	6.552(2)	13.906(3)
c/Å	17.448(2)	17.5513(7)	16.854(4)	19.107(5)	19.582(3)
β/°	91.730(9)	91.522(2)	90	96.48(2)	90
V/Å^3	984.8(2)	1000.48(6)	2158.6(9)	1101.0(5)	1464.9(5)
Z	2	2	4	4	4
D_c/g cm^{-3}	1.552	1.525	1.284	1.413	1.325
μ/mm^{-1}	0.813	0.707	0.723	0.099	0.094
F(000)	464	462	832	472	600
T/K	170(2)	120(2)	170(2)	293(2)	293(2)
θ Range/°	3.77–33.15	3.77–30.47	3.51–21.93	3.75–23.26	3.18–25.06
hkl Ranges	−7–8; ±15; −26–25	±7; −14–12, ±24	±11; −11–12; −17 −13	±9; -6–7; −21–20	−7–6; ±16; −19–14
Reflect. col./unique, R(int)	10663/3475	4250/2597	10446/1305	6054/1577	5457/1241
	0.0377	0.0275	0.1524	0.0531	0.0495
Completeness to θ	33.15 92.6%	30.47 85.4%	21.93 99.5%	23.26 99.7%	25.06 81.3%
Data/restr./param.	3475/6/158	2597/0/159	1305/0/137	1577/0/163	1486/0/200
Goodness-of-fit on F^2	1.052	1.034	1.362	1.066	0.929
Fin. R [$I > 2\sigma(I)$] $R1$; $wR2$	0.0363; 0.0941	0.0392; 0.0842	0.1222; 0.2384	0.0492; 0.1122	0.0400; 0.0549
Large. diff. peak and hole (e A^{-3})	0.606 and −0.354	0.361 and −0.676	0.674 and −0.411	0.157 and −0.143	0.104 and −0.102

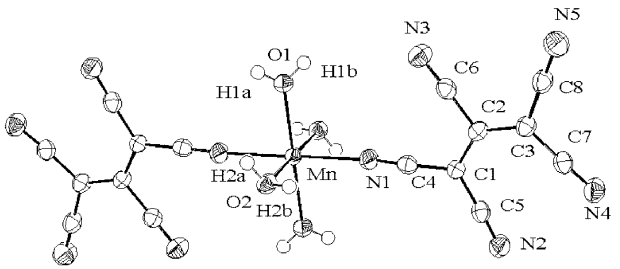

Fig. 1 ORTEP representation of the structure and atomic labeling scheme in compound **2**. Thermal ellipsoids are drawn at the 50% probability level.

of the *trans*-MN_2O_4 octahedral is slightly more important in the Mn derivative **2** than in the Fe derivative **1** with, in both cases, one of the MO bond, MO2, with a length essentially similar to that of the MN bond and the other MO bond shorter (Table 2). All bond lengths are close to those found in the isomorphic compounds $[M\{N(CN)_2\}_2(bpym)(H_2O)]$ (M = Fe, Mn; bpym = 2,2′-bipyrimidine) (bond lengths: FeN 2.097(4) and 2.125(5), FeO 2.126(4) Å, the equivalent bond lengths with Mn being *ca.* 0.05–0.07 Å longer).[29]

Despite the air sensitivity of compound $\mathbf{3}\cdot 0.5(CH_3)_2CO$ and the presence in the cell of disordered acetone, the crystal data collected are of sufficient quality allowing to get the main molecular features of the structure (see Experimental section). The crystals were analysed as belonging to the orthorhombic space group *Pbca*. The asymmetric unit consists of one metal atom lying on an inversion centre, one polynitrile in the general position and acetone (1/4 molecule) disordered around an inversion centre. The iron atom presents a pseudo-octahedral MN_6 coordination, the six nitrogen atoms arising from six different polynitrile units (Fig. 2). The FeN bond lengths, from 2.112(9) to 2.16(2) Å, are in agreement with a high spin Fe(II) ion.[30]

Table 2 Selected bond lengths (Å) and bond angles (°) for $[Fe(C_8N_5)_2(H_2O)_4]$ **1**, $[Mn(C_8N_5)_2(H_2O)_4]$ **2** and $[Fe(C_8N_5)_2]\cdot 0.5(CH_3)_2CO$ **3**

	1	2	3
M–N(1)	2.129(2)	2.205(1)	2.11(1)
M–O(1)	2.109(2)	2.144(1)	
M–O(2)	2.136(2)	2.224(1)	
Fe–N(4)			2.16(1)
Fe–N(5)			2.12(1)
C(1)–C(2)	1.408(2)	1.404(2)	1.37(2)
C(1)–C(4)	1.411(2)	1.419(2)	1.45(2)
C(1)–C(5)	1.418(2)	1.425(2)	1.42(2)
C(2)–C(3)	1.384(2)	1.389(2)	1.41(2)
C(2)–C(6)	1.456(2)	1.449(2)	1.47(2)
C(3)–C(7)	1.421(2)	1.422(2)	1.43(2)
C(3)–C(8)	1.426(2)	1.425(3)	1.40(2)
O(1)–M–N(1)	94.20(4)	94.80(5)	
O(1)–M–O(2)	91.54(4)	91.55(5)	
N(1)–M–O(2)	92.04(4)	92.49(5)	
N(1)–Fe–N(4)			93.4(3)
N(1)–Fe–N(5)			90.6(4)
N(4)–Fe–N(5)			91.2(3)
C(2)–C(1)–C(4)	118.7(2)	119.1(1)	121(1)
C(2)–C(1)–C(5)	124.0(2)	124.1(1)	124(1)
C(4)–C(1)–C(5)	117.2(2)	116.8(2)	115(2)
C(1)–C(2)–C(3)	129.8(2)	129.8(2)	130(2)
C(3)–C(2)–C(6)	115.4(2)	115.5(2)	115(1)
C(1)–C(2)–C(6)	114.8(2)	114.6(2)	115(2)
C(2)–C(3)–C(7)	123.0(2)	123.0(2)	123(1)
C(2)–C(3)–C(8))	120.2(2)	120.4(2)	121(1)
C(7)–C(3)–C(8	116.7(2)	116.4(2)	115(1)

The molecular structures. In complexes **1** and **2**, careful examination of the intermolecular distances clearly reveals a rich hydrogen bond system involving aqua and organocyanide ligands (Table 3). The resulting connections of independent molecules gives rise to a 3D array as shown in Fig. 3 for **2**. The shortest metal–metal distances match the crystallographic parameter *a* (5.40 Å).

In complex **3**, the poly bridging coordination mode of the pcp ligand affords a 3D structure arising exclusively from covalent bonds (Fig. 4). This leads to a 3D network in which each Fe atom is linked to four Fe as first neighbours and eight others as second neighbours (Fe···Fe distances 8.004 and 10.101/10.201 Å, respectively); the shortest Fe–Fe distances are associated to NCCCN bridges (N4–C7–C3–C8–N5), the other ones to NCCCCCN bridges (N1–C4–C1–C2–C3–C7/8–N4/5). The structure of **3** may be described as successive planes in the [001] direction. These planes perfectly contain the Fe ions in a roughly square arrangement; these ions [Fe···Fe interdistance *ca.* 8.0 Å] are linked by pcp ligands acting *via* their N1 and N2 atoms. These planes are linked by pcp ligands *via* their N5 atoms [interplanar Fe···Fe interdistance *ca.* 10.2 Å]. The crystal structure analysis reveals the presence of a distorted acetone molecule (see Experimental section); the relatively weak interactions between this molecule and the polynitrile unit (shortest intermolecular contacts around 3.5 Å) could explain the molecule disorder as well as the damage to the crystal on exposure to air.

The pcp ligands. As clearly described above, despite its five potentially bridging nitrile group, the pcp^- ligand shows only a monodentate coordination mode in compounds **1** and **2** and a μ_3-coordinating mode in compound **3**. Despite these differences, and although a pointed discussion of the structural parameters for **3** is not possible for the reason given above, this organic ligand roughly presents similar features in compounds **1–3**. In compounds **1** and **2**, the ligand is almost planar (maximum of deviation from mean plane for the N4 atom in **1**: −0.076 Å). The central C1C2C3 system, which obviously contains three sp^2 hybridised atoms, presents almost equivalent CC bonds in which the lengths (1.408(2) and 1.384(2) for **1**; 1.404(2) and 1.389(3) for **2**) indicate essentially similar degrees of multiplicity (Table 2). The electronic delocalisation affects the whole organic fragment as evidenced by four CC(N) bond lengths for the $C(CN)_2$ fragments in the range 1.41–1.43 Å and a central CC(N) bond length *ca.* 1.45 Å. The π system clearly also involves the CN groups for which it is noteworthy that, as usually observed with such polynitrile ligands, coordination does not deeply affect the CN bond length, the coordinated CN bond length [1.147(2) and 1.148(2) Å, respectively, for **1** and **2**] being close to those found for the uncoordinated ones [in the range 1.138(2)–1.146(2) and 1.150(2)–1.155(3) Å, respectively for **1** and **2**].

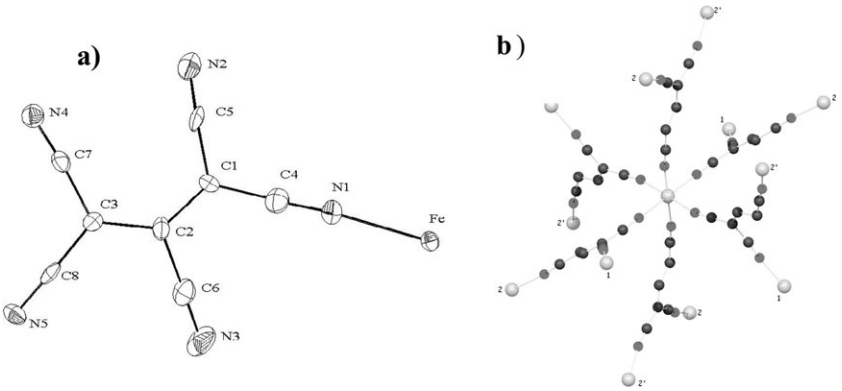

Fig. 2 (a) ORTEP representation with atoms shown at the 50% probability level and (b) the original μ_3-coordination of pcp ligand in compound **3**·0.5$(CH_3)_2CO$.

Magnetic and ESR measurements

The magnetic properties for compounds **1**, **2**, **3** and **4** (see Table 4) have been studied in the temperature range 2–300 K. These compounds present roughly similar behavior that are displayed in Fig. 5 as the thermal dependence of $\chi_m T$ product, where χ_m is the magnetic susceptibility per formula unit (1 mol of metal ion).

The room temperature $\chi_m T$ values (3.20, 4.32, 3.37 and 4.33 emu K mol^{-1} for **1**, **2**, **3** and **4**, respectively) are in good agreement with the expected values for magnetically isolated high-spin ions with $g = 2$ (3.0 emu K mol^{-1} for one high-spin Fe^{II} ion and 4.375 emu K mol^{-1} for one high-spin Mn^{II}, respectively). When cooling, the $\chi_m T$ products remain constant down to approximately 50 K for **1** and **2** and 100 K for **3** and **4**. Below these temperatures, the $\chi_m T$ products decrease, with a more pronounced decrease for **3** and **4** than for the hydrated compounds **1** and **2**, to reach values at 2 K of 2.0, 3.8, 0.68 and 1.50 emu K mol^{-1} for **1**, **2**, **3** and **4**, respectively (Fig. 5). These facts suggest the presence in the polymeric complexes **3** and **4** of antiferromagnetic interactions between the M(II) ions and indicate that the hydrated complexes **1** and **2** are essentially paramagnetic as expected from their monomeric structures. Although for the latter the smooth decreases at low temperature may be attributed to very weak antiferromagnetic interactions between M(II) ions through hydrogen bonds, attribution to a zero field splitting (ZFS) of isolated M(II) ions may not be excluded in all cases.[31] Since it is not possible to separate these two possible contributions, we attempted to fit the magnetic data of each compound using the two models, a simple Curie–Weiss law ($\chi_m = C/T - \theta$) and a ZFS.

Table 3 Hydrogen bond distances (Å) and angles (°) in compound **2**

D–H···A	D–H	H···A	D···A	DHA
O(1)–H(1a)···N(4)*	0.80(3)	2.09(3)	2.889(2)	174(3)
O(1)–H(1b)···O(2)**	0.84(3)	2.01(3)	2.827(2)	163(3)
O(2)–H(2a)···N(2)*	0.85(3)	1.99(3)	2.837(2)	174(3)
O(2)–H(2b)···N(3)***	0.84(3)	2.24(3)	2.926(2)	139(3)
O(2)–H(2b)···N(5)****	0.84(3)	2.38(3)	2.967(2)	127(3)

For the Fe compound **1**, the fit with a Curie–Weiss law ($C = 3.25(1)$ emu K^{-1} mol^{-1}, $g = 2.083(2)$, $\theta = -0.75(8)$ $K = -0.52(6)$ cm^{-1}) does not reproduce very well the low temperature data, indicating that the Fe(II) presents a ZFS that needs to be considered. Thus, we have fitted the magnetic susceptibility of this compound to an isolated $S = 2$ ion with a ZFS using the following equation.[32]

$$\chi = \frac{2\chi_{\|} + \chi_{\perp}}{3}$$

with

$$\chi_{\|} = \frac{Ng^2\mu_B^2}{kT}\frac{2e^{-x} + 8e^{-4x}}{1 + 2e^{-x} + 2e^{-4x}}$$

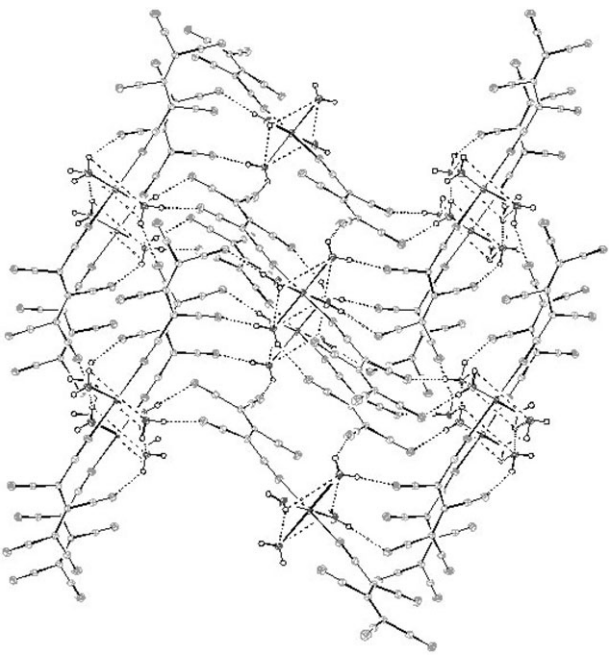

Fig. 3 Hydrogen bonding and packing diagram in compound **2** down the [100] plane.

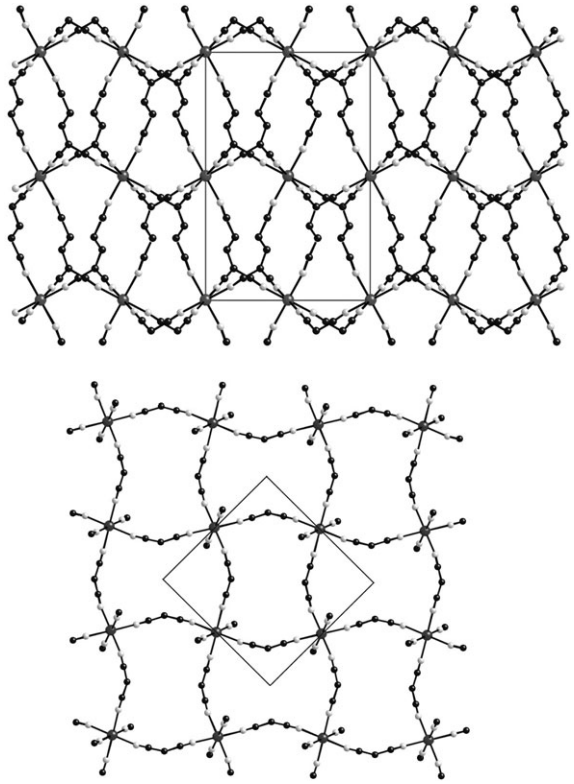

Fig. 4 Views of the 3D structure of compound $\mathbf{3}\cdot 0.5(CH_3)_2CO$. (a) Projection in the [001] direction. (b) Projection in the [010] direction.

And

$$\chi_{\perp} = \frac{Ng^2\mu_B^2}{kT}\frac{(6/x)(1-e^{-x}) + (4/3x)(e^{-x}-e^{-4x})}{1+2e^{-x}+2e^{-4x}}$$

where $x = |D|/kT$

This model reproduces very satisfactorily the magnetic data in the whole temperature range with the g and D values given in Table 5 (solid line in Fig. 5a). Note that the sign of D cannot be determined with powder magnetic measurements and note also that the D parameter may also account for the possible existence of weak antiferromagnetic interactions between the Fe(II) centers.

For the Mn compound **2**, the best fit (Fig. 5a) is provided by the Curie–Weiss law with the parameters given in Table 4. The low θ value accounts for the possible weak antiferromagnetic coupling between the complexes and/or the zero field splitting of the $S = 5/2$ Mn(II) ion.

Table 4 Magnetic data for compounds **1–4**

	C/emu K mol^{-1}	g	θ/K	θ/cm^{-1}	$\lvert D\rvert$/cm^{-1}
1[a]	—	2.079(3)	—	—	5.6(2)
2[b]	4.324(1)	1.988(1)	−0.303(2)	−0.211(1)	—
3[b]	3.450(6)	2.145(5)	−6.85(5)	−4.76(3)	—
4[b]	4.354(5)	1.995(3)	−3.77(2)	−2.62(2)	—

[a] Best fit obtained with a ZFS using equation for a spin ground state = 2. [b] Best fit obtained with a simple Curie–Weiss law.

For the non-hydrated complexes **3** and **4**, for which the structural data indicate a rather isotropic three dimensional structure, we have fitted the magnetic data with a simple Curie–Weiss law. This model reproduces very satisfactorily (Fig. 5b) the magnetic properties of both complexes with the parameters given in Table 4. In both cases, the small, although noticeable, negative θ values indicate the presence of weak antiferromagnetic interactions between the metal(II) ions through the pcp bridges. Note that other more complex models, such as the quadratic-layer antiferromagnet, do not produce better results.

At last, it is worthy to note that for compounds **1–4**, the spin ground states are confirmed with the isothermal magnetization at 2 K (Fig. 6) that can be well reproduced with a Brillouin function for $S = 2$ or $S = 5/2$ ground spin state with reduced g values that account for the weak antiferromagnetic interactions (solid line in Fig. 6).

ESR spectra have been recorded for the Mn compounds in various experimental conditions (powder and solution samples, r.t. and 150 K); as expected, in these conditions, the Fe compounds are silent. For derivatives **2** and **4**, the powder samples display at r.t. a broad and intense signal centred at $g = 2.007$ for **2** and $g = 2.010$ for **4**. The solution samples exhibit the hyperfine structure signal constituting six lines due to the interaction of the electrons with the nuclear spin of Mn ($I = 5/2$); the coupling constant values are $A_{Mn} = 94.2$ and 93.5 10^{-4} T for **2** and **4**, respectively. All these features are classical and in good agreement with those usually observed for derivatives including a Mn(II) ion in an octahedral environment.[33]

Crystal structure of the organic derivative 5

Reactions of the hexacyano-3,4-diazahexadienediide anion $[C_{10}N_8^{2-} = (NC)_2CC(CN)NNC(CN)C(CN)_2^{2-}]$ (Scheme 1)

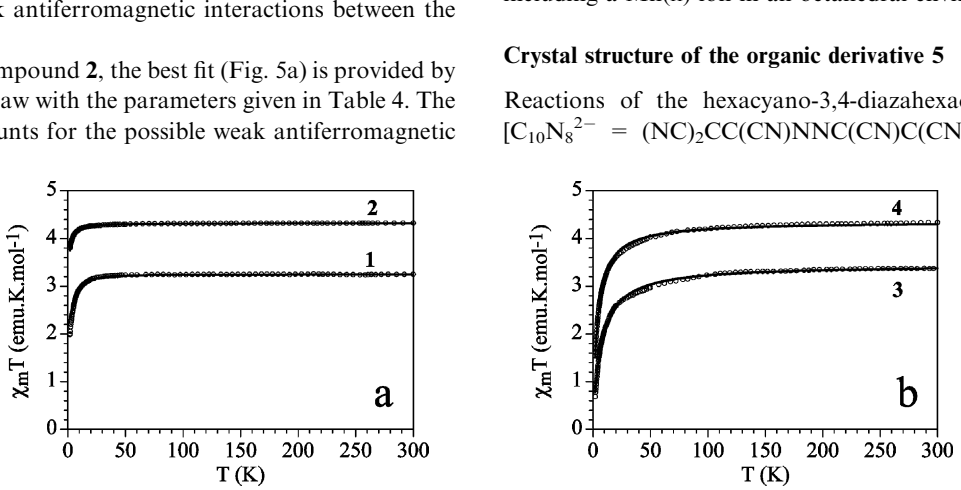

Fig. 5 Thermal variation of the $\chi_m T$ product for compounds **1–2** (a) and compounds **3–4** (b). Solid lines are the best fits to the ZFS model (compound **1**) or to the Curie–Weiss law (compounds **2**, **3** and **4**) (see text and Table 4).

Table 5 Selected bond lengths (Å) and bond angles (°) for **5** $C_{10}N_8H_2$ and **5**·$(CH_3)_2CO$

	5	**5**·$(CH_3)_2CO$
N(1)–C(1)	1.328(3)	1.337(4)
N(1)–C(4)	1.341(3)	1.343(4)
C(1)–N(4)	1.317(3)	1.330(3)
C(1)–C(2)	1.456(3)	1.458(4)
C(2)–C(3)	1.357(3)	1.343(4)
C(2)–C(7)	1.436(4)	1.430(5)
C(3)–N(2)	1.359(3)	1.358(3)
C(3)–C(8)	1.426(4)	1.446(5)
N(2)–N(3)	1.364(3)	1.369(3)
N(2)–C(4)	1.377(3)	1.383(3)
N(3)–C(5)	1.335(3)	1.345(4)
C(5)–C(6)	1.405(3)	1.402(4)
C(5)–C(9)	1.430(4)	1.427(5)
C(6)–C(4)	1.385(3)	1.394(4)
C(6)–C(10)	1.412(4)	1.409(5)
C(1)–N(1)–C(4)	117.5(2)	116.4(3)
N(4)–C(1)–N(1)	119.0(2)	118.2(3)
N(4)–C(1)–C(2)	119.8(2)	119.5(3)
N(1)–C(1)–C(2)	121.1(2)	121.7(4)
C(3)–C(2)–C(7)	120.2(2)	120.8(4)
C(3)–C(2)–C(1)	119.2(2)	119.0(3)
C(7)–C(2)–C(1)	120.7(2)	120.1(4)
C(2)–C(3)–N(2)	118.3(2)	118.6(3)
C(2)–C(3)–C(8)	124.3(2)	124.4(3)
N(2)–C(3)–C(8)	117.5(2)	117.0(4)
C(3)–N(2)–N(3)	124.9(2)	124.4(3)
C(3)–N(2)–C(4)	120.5(2)	120.8(3)
N(3)–N(2)–C(4)	114.5(2)	114.7(3)
C(5)–N(3)–N(2)	102.0(2)	101.4(3)
N(3)–C(5)–C(6)	113.8(2)	114.6(3)
N(3)–C(5)–C(9)	120.7(2)	119.2(4)
C(6)–C(5)–C(9)	125.5(2)	126.3(4)
C(4)–C(6)–C(5)	105.0(2)	104.6(3)
C(4)–C(6)–C(10)	127.5(2)	129.2(4)
C(5)–C(6)–C(10)	127.6(2)	126.0(3)
N(1)–C(4)–N(2)	123.3(2)	123.1(3)
N(1)–C(4)–C(6)	132.0(2)	132.1(4)
N(2)–C(4)–C(6)	104.7(2)	104.7(4)

with the metal complexes $[M(CH_3CN)_n](BF_4)_2$ (M = Mn, Fe, Ni and Cu) did not afford polynitrile metal complexes but contributed to a new organic derivative **5**, of formula $C_{10}N_8H_2$.

Crystallisation of compound **5** in dichloromethane affords small yellow cubic crystals of **5** which were analysed as crystallising in the monoclinic space group $P2_1/n$; similar

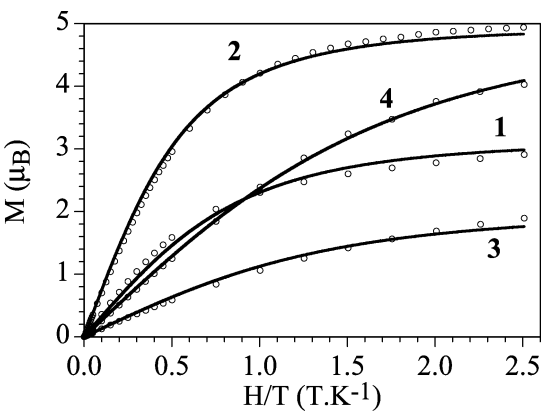

Fig. 6 Isothermal magnetization at 2 K of the compounds **1–4**. Solid lines represent the best fits to the Brillouin function (see text).

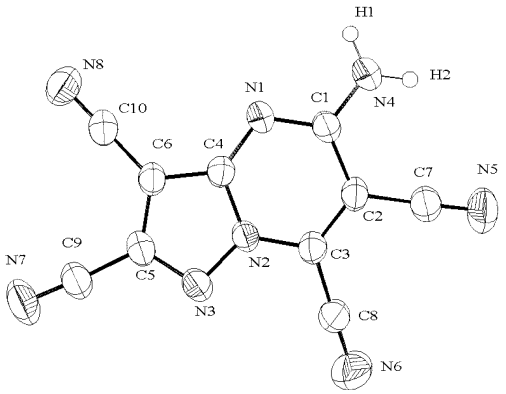

Fig. 7 Structure and atomic labeling scheme in compound **5**. Thermal ellipsoids are drawn at the 50% probability level.

crystallisation in acetone produced needle-shape yellow crystals of **5**·$(CH_3)_2CO$ which crystallised in the orthorhombic space group $P2_12_12_1$. Both structures contain essentially similar $C_{10}N_8H_2$ units but differ strongly in the relative arrangement of these units in the solid state (Table 5).

The organic $C_{10}N_8H_2$ molecule is bicyclic and built on an pyrazolo[1,5-*a*] pyrimidine skeleton (Fig. 7). Both cycles bear substituents; the pyrimidine cycle holds two cyano groups and one amino group and the pyrazole cycle two cyano groups. The bicyclic skeleton is planar (maximum of deviation to the mean-square plane: 0.03 Å for C6) and the whole molecule is essentially planar (maximum of deviation to the mean-square plane: 0.1 Å for N8). Within the two rings, the CC bond length distances are in the range 1.357(3)–1.456(4) Å, while the CN distances vary from 1.328(4) to 1.383(3) Å (Table 5). The diaza N2N3 bond length (1.364(3) and 1.369(3) Å for **5**. and **5**·$(CH_3)_2CO$, respectively) is very close to that found in the starting anion $[C_{10}N_8]^{2-}$ (1.372(4) Å).[12] Both are smaller than NaNb single bond lengths (*ca*. 1.40 Å with Na and Nb planar and 1.45 Å with Na and Nb pyramidal),[34] indicating that the NN bond also possesses some character of multiplicity.[33] In the pyrimidine cycle, the angle bond values close to 120° agree well with hybridised sp^2 atoms, while in the pyrazole ring, due to the usual constraints of a five-membered ring, these values deviate from 120° varying from 101 to 132°. All these features indicate an important delocalization of the π system on the bicycle skeleton; this delocalization also affects the substituents as shown by the short CC(N) bond lengths (from 1.412 to

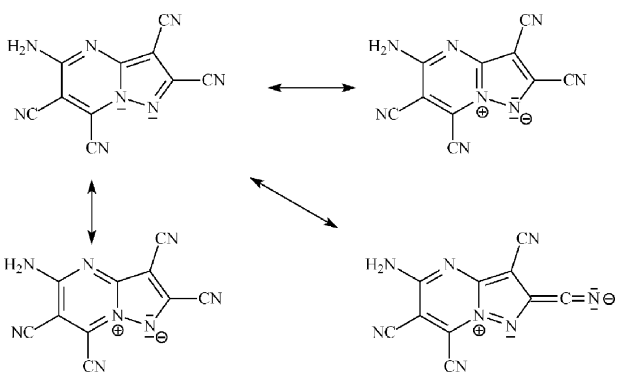

Scheme 2 Resonance forms for **5**.

Table 6 Hydrogen bond distances (Å) and angles (°) in compound **5** (a) and in compound **5** · acetone (b)

D–H···A	D–H	H···A	D···A	DHA
(a)				
N(4)–H(2)···N(7)[a]	0.86	2.19(3)	2.974(3)	151.3
N(4)–H(1)···N(8)[b]	0.86	2.19(3)	3.039(3)	169.1
(b)				
N(4)–H(4A)···O(23)[c]	0.86	2.09	2.877(4)	152.6
N(4)–H(4B)···N(8)[c]	0.86	2.01	3.099(4)	153.2

[a] $x+1, y-1, z$. [b] $-x+1, -y, -z$. [c] $-x+3/2, -y, z+1/2$.

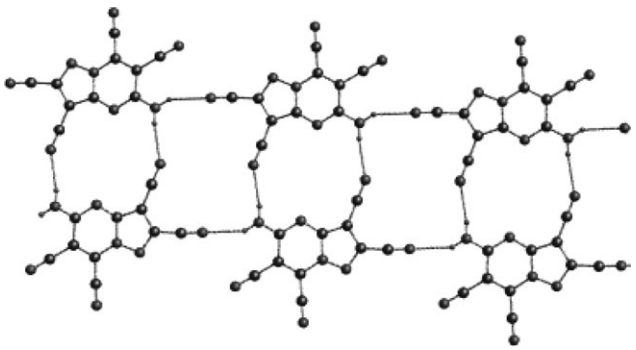

Fig. 8 Hydrogen bonding in compound **5**: formation of linear double chains.

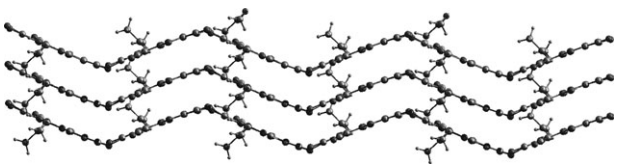

Fig. 9 Hydrogen bonding in compound **5** · $(CH_3)_2CO$: formation of zig-zag chains.

1.436 Å) and a CNH_2 bond length shorter than usual Csp^2N single bond length. All these features (planarity, bond length and bond angle values) suggest several resonance forms for **5** (Scheme 2), which presents an overall geometry not significantly different from previous related derivatives.[35]

In the monoclinic compound **5**, intermolecular hydrogen bonds based on the hydrogen atoms of the NH_2 group of one $C_{10}H_2N_8$ unit with the nitrogen atoms N7 and N8 of the cyano groups of two different adjacent $C_{10}H_2N_8$ units lead to formation of linear double chains (Table 6, Fig. 8); these chains stack with an interstack distance of 3.54 Å. In the orthorhombic compound **5** · $(CH_3)_2CO$, the intermolecular bond system is more complicated since the acetone molecule also contributes to the hydrogen bonding by its oxygen atom. This leads to zig-zag chains (Table 6, Fig. 9).

The formation of this bicyclic derivative from reaction of the non-cyclic $[C_{10}N_8]^{2-}$ anion with a transition metal complex might arise from a mechanism which successively involves (Scheme 3) (i) weak coordination of the polynitrile unit to the metal *via* one of its N atoms (this induces a decrease of the electronic density on the corresponding C atom), (ii) after rotation about the NN bond, nucleophilic attack on this C atom of one of the NC groups of the second $C(CN)_2$ wing affording, *via* a concerted mechanism, the bicycle skeleton and (iii) decomplexation with protonation of the coordinated nitrogen atom. This formation corroborates previous studies showing that cumulated diaza derivatives are excellent synthons for a variety of fused pyrazolo heterocycles.[36]

Conclusion

In this study, a pentacyanopropenido complex **3** has been characterised. It displays an unprecedented 3D structure arising from an unusual μ_3-coordination mode for the organocyanide ligand. As expected, within this new polymeric network, antiferromagnetic interactions take place between the metallic centres due to the bridging ligand role. It is worth noting that these interactions, even weak, are more important compared to those for hydrated complexes **1** and **2** for which a rich hydrogen bond system also generates a 3D array. Attempts to generate similar architectures, starting from the hexacyano-3,4-diazahexadienediide anion, were unsuccessful, but the synthesis of the new organic derivative **5**, due to its

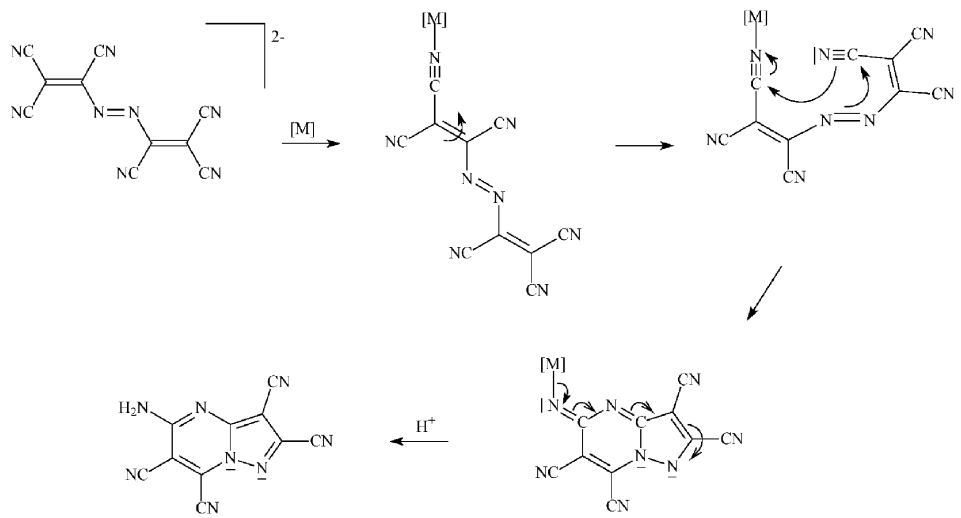

Scheme 3 Mechanism for the formation of compound **5**.

geometrical and electronic features (a π electronic system, several cyano groups), opens new perspectives for the development of organocyanide chemistry.

Acknowledgements

The authors gratefully acknowledge the CNRS (Centre National de la Recherche Scientifique) and UMR 6521. E. L. thanks the French "Ministère de l'Education Nationale, de la Recherche et de la Technologie" for a thesis grant.

References

1 (*a*) E. Coronado, P. Delhaès, D. Gatteschi and J. S. Miller, *Molecular Magnetism: From Molecular Assemblies to the Devices*, Kluwer Academic Publishers, Dordrecht, The Netherlands, 1996; (*b*) J. S. Miller and M. Drillon, *Magnetism: Molecules to Materials*, Wiley-VCH, Weinheim, vol. V, 2005.

2 (*a*) J. M. Manriquez, G. T. Yee, R. S. McLean, A. J. Epstein and J. S. Miller, *Science*, 1991, **252**, 1415; (*b*) J. S. Miller, *Inorg. Chem.*, 2000, **39**, 4392; (*c*) J. S. Miller and J. L. Manson, *Acc. Chem. Res.*, 2001, **34**, 563; (*d*) J. L. Manson, in *Magnetism Molecules to Materials*, ed. J. S. Miller and M. Drillon, Wiley-VCH, Weinheim, Germany, 2005, vol. V, p. 71; (*e*) J. L. Manson, E. Ressouche and J. S. Miller, *Inorg. Chem.*, 2000, **39**, 1135; (*f*) C. R. Kmety, Q.-Z. Huang, J. W. Lynn, R. W. Erwin, J. L. Manson, S. McCall, J. E. Crow, K. L. Stevenson, J. S. Miller and A. J. Epstein, *Phys. Rev. B*, 2000, **62**, 5576; (*g*) M. R. Pederson, A. Y. Liu, T. Baruah, E. Z. Kurmaev, A. Moewes, S. Chiuzbaian, M. Neumann, C. R. Kmety, K. L. Stevenson and D. Ederer, *Phys. Rev. B*, 2002, **66**, 014446/1; (*h*) R. Feyerherm, A. Loose and J. L. Manson, *J. Phys.: Condens. Matter*, 2003, **15**, 663; (*i*) R. Plachy, K. I. Pokhodnya, P. C. Taylor, J. Shi, J. S. Miller and A. J. Epstein, *Phys. Rev. B*, 2004, **70**, 064411/1; (*j*) D. Haskel, Z. Islam, J. Lang, C. Kmety, G. Srajer, K. I. Pokhodnya, A. J. Epstein and J. S. Miller, *Phys. Rev. B*, 2004, **70**, 054422/1; (*k*) J. A. Schlueter, J. L. Manson, K. A. Hyzer and U. Geiser, *Inorg. Chem.*, 2004, **43**, 4100; (*l*) R. Feyerherm, A. Loose, S. Landsgesell and J. L. Manson, *Inorg. Chem.*, 2004, **43**, 6633; (*m*) J. A. Schlueter, J. L. Manson and U. Geiser, *Inorg. Chem.*, 2005, **44**, 3194.

3 (*a*) K. R. Dunbar, *Angew. Chem., Int. Ed. Engl.*, 1996, **35**, 1659; (*b*) P. S. Szalay, J.-R. Galan-Mascaros, B. L. Schottel, J. Bacsa, L. M. Perez, A. S. Ichimura, A. Chouai and K. R. Dunbar, *J. Cluster Sci.*, 2004, **15**, 503; (*c*) H. Zhao, J. Basca, A. Prosvirin, N. Lopez and K. R. Dunbar, *Polyhedron*, 2005, **24**, 1907.

4 (*a*) W. Kaim and M. Moscherosch, *Coord. Chem. Rev.*, 1994, **129**, 157; (*b*) H. Hartmann, W. Kaim, M. Wanner, A. Klein, S. Frantz, C. Duboc-Toia, J. Fiedler and S. Zalis, *Inorg. Chem.*, 2003, **42**, 7018; (*c*) A. N. Maity, B. Schwederski and W. Kaim, *Inorg. Chem. Commun.*, 2005, **8**, 600.

5 (*a*) S. R. Batten and K. S. Murray, *Coord. Chem. Rev.*, 2003, **246**, 103; (*b*) M. Kurmoo and C. J. Kepert, *New J. Chem.*, 1998, **22**, 1515; (*c*) S. R. Batten, P. Jensen, C. J. Kepert, M. Kurmoo, B. Moubaraki, K. S. Murray and D. J. Price, *J. Chem. Soc., Dalton Trans.*, 1999, **12**, 2987; (*d*) A. Lappas, A. S. Wills, M. A. Green, K. Prassides and M. Kurmoo, *Phys. Rev. B*, 2003, **67**, 144406/1; (*e*) P. M. van der Werff, S. R. Batten, P. Jensen, B. Moubaraki, K. S. Murray and J. D. Cashion, *Cryst. Growth Des.*, 2004, **4**, 503; (*f*) S. R. Batten, J. Bjernemose, P. Jensen, B. A. Leita, K. S. Murray, B. Moubaraki, J. P. Smith and H. Toftlund, *Dalton Trans.*, 2004, 3370; (*g*) P. M. van der Werff, E. Martinez-Ferrero, S. R. Batten, P. Jensen, C. Ruiz-Perez, M. Almeida, J. C. Waerenborgh, J. D. Cashion, B. Moubaraki, J. R. Galan-Mascaros, J. M. Martinez-Agudo, E. Coronado and K. S. Murray, *Dalton Trans.*, 2005, 285.

6 (*a*) C. Kremer, C. Melián, J. Torres, M. P. Juanicó, C. Lamas, H. Pezaroglo, E. Manta, H. Schumann, J. Pickardt, F. Girgsdies, O. N. Ventura and F. Lloret, *Inorg. Chim. Acta*, 2001, **314**, 83; (*b*) E. Colacio, F. Lloret, I. Ben Maimoun, R. Kivekaes, R. Sillanpaeae and J. Suarez-Varela, *Inorg. Chem.*, 2003, **42**, 2720; (*c*) J. Carranza, J. Sletten, F. Lloret and M. Julve, *Inorg. Chim. Acta*, 2004, **357**, 3304; (*d*) E. Colacio, I. Ben Maimoun, F. Lloret and J. Suarez-Varela, *Inorg. Chem.*, 2005, **44**, 3771.

7 W. J. Middleton, E. L. Little, D. D. Coffman and V. A. Engelhardt, *J. Am. Chem. Soc.*, 1958, **80**, 2795.

8 (*a*) T. L. Cairns, R. A. Carboni, D. D. Coffman, V. A. Engelhardt, R. E. Heckert, E. L. Little, E. G. McGeer, B. C. McKusick, W. J. Middleton, R. M. Scribner, C. W. Theobald and H. E. Winberg, *J. Am. Chem. Soc.*, 1958, **80**, 2775; (*b*) R. E. Merrifield and W. D. Phillips, *J. Am. Chem. Soc.*, 1958, **80**, 2778; (*c*) W. J. Middleton, R. E. Heckert, E. L. Little and C. G. Krespan, *J. Am. Chem. Soc.*, 1958, **80**, 2783; (*d*) W. J. Middleton and V. A. Engelhardt, *J. Am. Chem. Soc.*, 1958, **80**, 2788; (*e*) B. C. McKusick, R. E. Heckert, T. L. Cairns, D. D. Coffman and H. F. Mower, *J. Am. Chem. Soc.*, 1958, **80**, 2806; (*f*) G. N. Sausen, V. A. Engelhardt and W. J. Middleton, *J. Am. Chem. Soc.*, 1958, **80**, 2815; (*g*) W. J. Middleton, V. A. Engelhardt and B. S. Fisher, *J. Am. Chem. Soc.*, 1958, **80**, 2822; (*h*) T. L. Cairns and B. C. McKusick, *Angew. Chem.*, 1961, **73**, 520; (*i*) O. W. Webster, W. Mahler and R. E. Benson, *J. Am. Chem. Soc.*, 1962, **84**, 3678; (*j*) L. R. Melby, R. J. Harder, W. R. Hertler, W. Mahler, R. E. Benson and W. E. Mochel, *J. Am. Chem. Soc.*, 1962, **84**, 3374.

9 M. Decoster, J. E. Guerchais, Y. Le Mest, J. Sala-Pala, S. Triki and L. Toupet, *Polyhedron*, 1996, **15**, 195.

10 (*a*) S. Triki, J. Sala-Pala, M. Decoster, P. Molinié and L. Toupet, *Angew. Chem., Int. Ed.*, 1999, **38**, 113; (*b*) F. Thétiot, S. Triki, J. Sala-Pala and C. J. Gomez-Garcia, *Synth. Met.*, 2005, **153**, 481; (*c*) F. Thétiot, S. Triki, J. Sala-Pala and S. Gohlen, *Inorg. Chim. Acta*, 2005, **358**, 3277; (*d*) S. Triki, F. Thétiot, F. Vandevelde, J. Sala-Pala and C. J. Gomez-Garcia, *Inorg. Chem.*, 2005, **44**, 4086.

11 B. Le Gall, F. Conan, N. Cosquer, J.-M. Kerbaol, J. Sala-Pala, M. M. Kubicki, E. Vigier, C. J. Gomez-Garcia and P. Molinié, *Inorg. Chim. Acta*, 2005, **358**, 2513.

12 M. Decoster, F. Conan, M. Kubicki, Y. Le Mest, P. Richard, J. Sala-Pala and L. Toupet, *J. Chem. Soc., Perkin Trans. 2*, 1997, 265.

13 S. Duclos, F. Conan, S. Triki, Y. Le Mest, M. L. Gonzalez and J. Sala-Pala, *Polyhedron*, 1999, **18**, 1935.

14 (*a*) F. Thétiot, S. Triki, J. Sala-Pala and C. J. Gomez-Garcia, *J. Chem. Soc., Dalton Trans.*, 2002, 1687; (*b*) F. Thétiot, S. Triki and J. Sala-Pala, *Polyhedron*, 2003, **22**, 1837; (*c*) J. R. Galan-Mascaros, F. Thétiot, S. Triki, J. Sala-Pala and K. R. Dunbar, *J. Phys. IV*, 2004, **114**, 625; (*d*) F. Thétiot, S. Triki, J. Sala-Pala, J. R. Galan-Mascaros and K. R. Dunbar, *Eur. J. Inorg. Chem.*, 2004, 3783.

15 (*a*) G. A. Sim, D. I. Woodhouse and G. R. Knox, *J. Chem. Soc., Dalton Trans.*, 1979, 629; (*b*) W. P. Jensen and R. A. Jacobson, *Inorg. Chim. Acta*, 1981, **50**, 189; (*c*) V. Bertolasi and G. Gilli, *Acta Crystallogr., Sect. C: Cryst. Struct. Commun.*, 1983, **C39**, 124; (*d*) J. S. Miller, J. C. Calabrese, H. Rommelmann, S. R. Chittipeddi, J. H. Zhang, W. M. Reiff and A. J. Epstein, *J. Am. Chem. Soc.*, 1987, **109**, 769; (*e*) S. Barlow and D. O'Hare, *Acta Crystallogr., Sect. C: Cryst. Struct. Commun.*, 1996, **C52**, 578; (*f*) W. Chen, H. Li, Z. J.- Zhong, K. Zhang and X.-Z. You, *Acta Crystallogr., Sect. C: Cryst. Struct. Commun.*, 1996, **C52**, 3030.

16 (*a*) T. J. Johnson, K. W. Hipps and R. D. Willett, *J. Phys. Chem.*, 1988, **92**, 6892; (*b*) K. W. Hipps, U. Geiser, U. Mazur and R. D. Willett, *J. Phys. Chem.*, 1984, **88**, 2498.

17 M. I. Bruce, R. C. Wallis, B. W. Skelton and A. H. White, *J. Chem. Soc., Dalton Trans.*, 1981, 2205.

18 L. Jäger, C. Tretner, K. Sünkel and J. Kozisek, *Z. Anorg. Allg. Chem.*, 1997, **624**, 1381.

19 A. Dvorsky, J. Kozisek, L. Jäger and C. Tretner, *Acta Crystallogr., Sect. C: Cryst. Struct. Commun.*, 1997, **C53**, 556.

20 L. Jäger, C. Wagner and W. Hanke, *J. Mol. Struct.*, 2000, **525**, 107.

21 M. L. Yates, A. M. Arif, J. L. Manson, B. A. Kalm, B. M. Burkhart and J. S. Miller, *Inorg. Chem.*, 1998, **37**, 840.

22 B. J. Hattaway, D. G. Hola and A. E. Underhill, *J. Chem. Soc.*, 1962, 2444.

23 W. Otwinowski and Minor, *Methods Enzymol.*, 1997, **276**, 307.

24 G. M. Sheldrick, *SHELXS and SHELXL-97*, University of Göttingen, Göttingen, Germany.

25 CrysAlis RED, Oxford Diffraction Ltd., Abingdon, Oxfordshire, UK, 2003.

26 A. Altomare, M. C. Burla, M. Camalli, G. L. Cascarano, C. Giacovazzo, A. Guagliardi, A. G. G. Moliterni, G. Polidori and R. Spagna, *J. Appl. Crystallogr.*, 1999, **32**, 115–119.

27 L. J. Farrugia, *J. Appl. Crystallogr.*, 1999, **32**, 837.
28 M. I. Bruce, M. A. Buntine, K. Costuas, B. J. Ellis, J. F. Halet, P. J. Low, B. W. Skelton and A. H. White, *J. Organomet. Chem.*, 2004, **689**, 3308.
29 S. R. Marshall, C. D. Incarvito, J. L. Manson, A. L. Rheingold and J. S. Miller, *Inorg. Chem.*, 2000, **39**, 1969.
30 P. Guionneau, M. marchivie, G. Bravic, J. F. Létard and D. Chasseau, *Top. Curr. Chem.*, 2004, **234**, 97.
31 O. Kahn, *Molecular Magnetism*, VCH Publishers, New York, USA, 1993.
32 C. J. O'Connor, *Prog. Inorg. Chem.*, 1982, **29**, 203.
33 F. E. Mabbs and D. Collison, *Studies in Inorganic Chemistry: Electron Paramagnetic Resonance of Transition Metal Compounds*, Elsevier, Amsterdam, The Netherlands, 1992, vol. 16.
34 F. H. Allen, O. Kennard, D. G. Watson, L. Brammer, A. J. Orpen and R. Taylor, *J. Chem. Soc., Perkin Trans. 2*, 1987, S1.
35 (*a*) E. E. Schweizer, J. E. Hayes, A. L. Rheingold and W. Xu, *J. Org. Chem.*, 1987, **52**, 1810; (*b*) S. Chimichi, B. Cosimelli, F. Bruni, S. Selleri, A. Costanzo, G. Guerrini and G. Valle, *J. Chem. Soc., Perkin Trans. 2*, 1994, 1657.
36 (*a*) E. E. Schweizer and S. Evans, *J. Org. Chem.*, 1978, **43**, 4328; (*b*) X.-L. Ren, C. Wu, Y. Gao, X.-M. Zou, H.-Z. Yang and Jiegou Huaxue, *Chin. J. Struct. Chem.*, 2004, **23**, 267; (*c*) E. E. Schweizer, W. Hsueh, A. L. Rheingold and R. L. Durney, *J. Org. Chem.*, 1983, **48**, 3889; (*d*) E. E. Schweizer and K. J. Lee, *J. Org. Chem.*, 1984, **49**, 1959; (*e*) E. E. Schweizer and K. J. Lee, *J. Org. Chem.*, 1984, **49**, 1964; (*f*) G. Zvilivhovsky and V. Gurvich, *J. Chem. Soc., Perkin Trans. 1*, 1995, 2509.

